Quasi-zero stiffness magnetic levitation vibration isolation system with improved passive stability: A theoretical analysis

Nur Afifah Kamaruzaman, William S. P. Robertson, Mergen H. Ghayesh, Benjamin S. Cazzolato, and Anthony C. Zander

School of Mechanical Engineering, The University of Adelaide, 5005 SA, Australia

ABSTRACT

This paper presents a theoretical analysis of a planar quasi-zero stiffness magnetic levitation system with improved passive rotational stability for the application of vibration isolation. Through proper choices of equilibrium position and magnet geometry (horizontal gap parameter), the system is made stable in the vertical and rotational degrees of freedom, thus requiring active stability control only in the horizontal degree of freedom. It is found that the control effort is inversely proportional to the magnitude of the passive rotational stability. The effect of these parameters on the stability and vibration response of the system is examined. The nonlinearity of the system is also investigated by comparing the vibration response to its linear representation, in which it is shown that the system becomes increasingly nonlinear as it is perturbed further away from its equilibrium position.

1 INTRODUCTION

The nonlinearity of quasi-zero stiffness (QZS) isolators allows the attainment of low dynamic stiffness for good vibration isolation performance and high static stiffness for large load bearing. Using magnetic spring rather than physical springs to create these characteristics is advantageous due to the lack of friction, buckling effects, and vibration transmission via parasitic higher order modes. However, levitation between permanent magnets cannot be held in equilibrium as at least one translational axis would be unstable (Bassani, 2006a; Earnshaw, 1839). Thus, stable contactless magnetic levitation can only be achieved with the integration of active control.

It is desired to minimise the use of active control as it requires power and generates noise due to the sensitivity and precision of sensors. Proper selection of operating position and magnet geometry can reduce the inherent instability of a magnetic spring, thus reducing the need for active stability controllers. Bassani (2006b) observed that the instability between a pair of axially magnetised ring magnets can be reduced significantly via appropriate eccentricity and gap. Similarly, a six-degree of freedom (DOF) isolation table was made passively stable in five DOFs through proper design, thus only requiring active control in a single DOF (Choi et al., 2003). Additionally, Robertson (2013) found that a rotationally-unstable spring can be stabilised by integrating lever arms through the addition of weak magnets. While the concept of reducing passive instability of a magnetic spring has been demonstrated, it has not been thoroughly examined for the application of vibration isolation.

In related work, we have previously modified the design of a QZS magnetic spring by integrating lever arms to balance the rotational DOF (Kamaruzaman et al., forthcoming). Static and dynamic simulations indicate that the lever arm is advantageous in improving the rotational stability of the system, thus reducing the active control effort required to achieve stable levitation. The studies however exclude the effect of base excitation. It is anticipated that the stability of the system will be affected by base excitation, especially at resonance. In the present work, we extend the investigation of the influence of the lever arm on the vibration isolation performance by exciting the base of the system with multiple types of signal. The vibration isolation performance of the system is examined via its transmissibility, calculated using computational dynamical analysis.

2 DESIGN AND THEORY OF MAGNETIC SPRING WITH IMPROVED PASSIVE ROTATIONAL STABILITY

Figure 1 shows the schematic of the planar magnetic spring with quasi-zero stiffness characteristics. The top magnet pair in attraction functions as a passive gravity compensator to support large load, while the bottom magnet pairs in repulsion provide softening characteristics for stiffness reduction. A change in the vertical force of the spring due to displacement can be approximated by a quadratic polynomial (Robertson et al., 2009), in which the vertex corresponds to the point of zero stiffness.

The passive rotational stability of the system is manipulated by a parameter referred to as the normalised horizontal gap *p* (Kamaruzaman et al., forthcoming). Note that the gap *p* is equal to the non-normalised horizontal gap *cp* divided by the face size width *c* of the bottom magnets (i.e., $p = cp/c$). Ideally, with a non-zero gap *p*, the spring is balanced along the rotational β direction provided that the spring is centred (vertically symmetric) as equal clockwise and counter-clockwise torques are produced. In this paper and related-work (Kamaruzaman et al., forthcoming), grade N35 cuboid magnets are used with a 50mm length into the page, face size width *a* = 50mm for the top magnet pair, *c* = 25mm for the bottom magnet pairs, height *b* = 20mm, distance 2*bd* between the centre of the fixed and levitating magnets (*d* = 2.5), and distance *be* between the centre of the levitating magnets (*e* = 2).

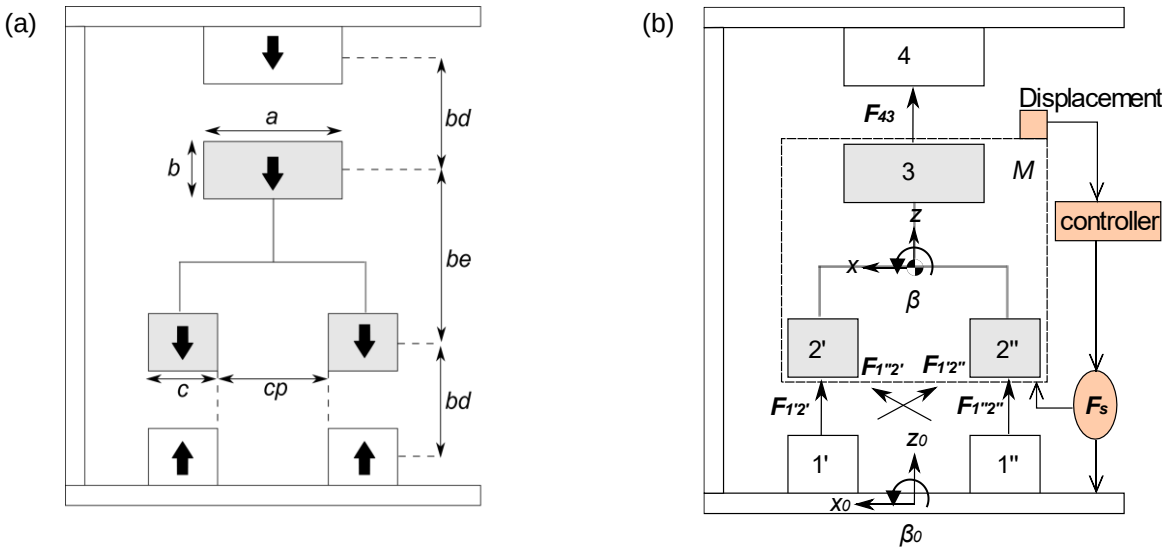

Figure 1: Schematic of a planar quasi-zero stiffness magnetic spring with adjustable passive rotational stability (via the normalised horizontal gap *p*). (a) Geometry of the magnet spring with large arrows indicate magnetisation direction. (b) Forces between the permanent magnets and active (stability) control ***Fs***.

Forces between cuboid permanent magnets with parallel magnetisation can be calculated analytically using the solution provided by Akoun and Yonnet (1984). Using superposition principle, the total force of the spring is given by

$$\boldsymbol{F} = \boldsymbol{F}_{1'2'} + \boldsymbol{F}_{1''2''} + \boldsymbol{F}_{1''2'} + \boldsymbol{F}_{1'2''} + \boldsymbol{F}_{43}, \tag{1}$$

where the first four terms constitute for repulsive forces and the last term represents attractive forces for each magnet pair as shown in Figure 1(b). For the calculation of torques, the lever arm is defined as the perpendicular distance from the marked centre of rotation to the point (centre of magnets) which force is applied. The cross-product of the lever arms and the forces gives the torques. Due to a restriction that the magnet sides must remain parallel to each other as a consequence of using such analytical force solution, a small angle approximation is made (Robertson, Cazzolato, and Zander, 2012). The stiffness is calculated from the gradient of either the force or moment when a small translation or rotation is applied to the levitating assembly, accordingly.

3 INFLUENCE OF HORIZONTAL GAP

This section outlines the influence of the horizontal gap *p* on static and dynamic stabilities, as well as the vibration isolation performance of the system. Positive and negative stiffness indicates stability and instability, respectively.

3.1 Static analysis

In our previous work, it was found that the load bearing force at the quasi-zero stiffness position slightly decreases with the gap *p* – caused by the loss of magnetic interactions (***F1'2"*** and ***F1"2'***) as the magnets move further away from one another. Consequently, this shifts the QZS position closer towards the bottom fixed magnets.

As shown in Figure 2(a), the horizontal gap *p* (for gap $p \geq 1$) proves to be advantageous in stabilising the initially unstable rotational β DOF (gap of $p = 0$) when the spring is horizontally constrained at the centre while being displaced vertically. This also applies for a range of horizontal *x* displacement. Figure 2(b) shows the rotational stiffness $k_{\beta\beta}$ of the spring due to horizontal *x* displacement upon levitating 10 mm below the QZS position (vertically stable). In both cases, a larger gap *p* appears to be favourable for achieving high passive rotational stability. However, beyond a certain horizontal *x* displacement (indicated by the shaded regions in Figure 2(b)), a larger gap *p* imposes greater adverse effects on the rotational stability.

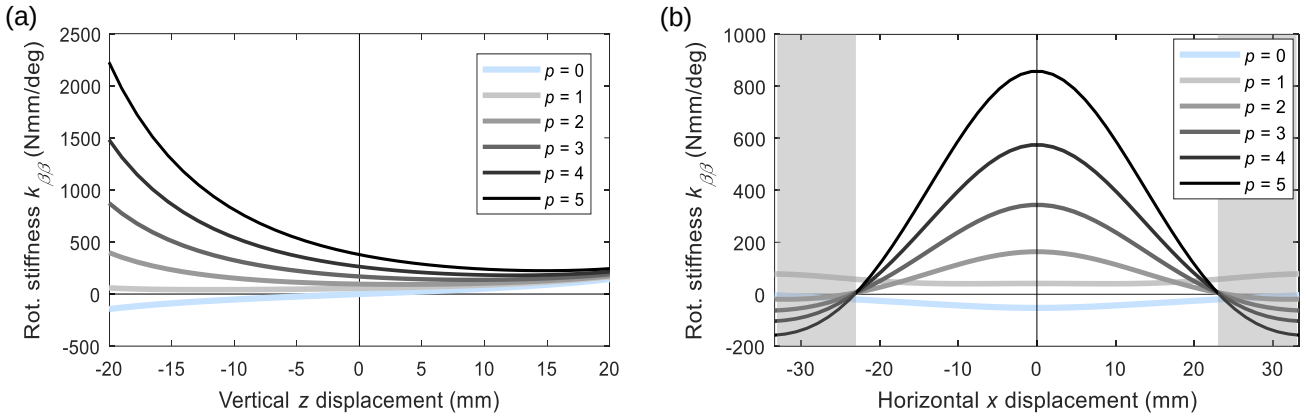

Source (Kamaruzaman et al., forthcoming)

Figure 2: Influence of horizontal gap *p* on the rotational static stability of the system. (a) Rotational stiffness $k_{\beta\beta}$ due to vertical *z* displacement. (b) Rotational stiffness $k_{\beta\beta}$ due to horizontal *x* displacement. The shaded regions indicate rotational instability for gap of p > 1.

The stiffness characteristics of the translational DOFs are largely unaffected by the gap *p*, which is desirable as to maintain a wide effective bandwidth of vibration isolation. In general, vibration attenuation only occurs beyond the marginal frequency $\omega_c = \sqrt{2k/m}$; thus, in order to isolate a fixed mass *m* from vibration at very low frequencies, the stiffness *k* must be kept small (i.e., close to zero).

3.2 Dynamic analysis

To analyse the effect of the horizontal gap *p* on the dynamic stability of the spring and ultimately the vibration isolation performance, multiple cases of dynamic simulation are investigated: (1) initial perturbation (vertical *z* DOF) from the equilibrium position with no base excitation; (2) 1-DOF swept sine and tonal base excitation; (3) 3-DOF uniform random base excitation.

In general, the equations of motion of the levitating assembly are defined as

$$\begin{aligned} M\ddot{z} &= -Mg + F_z(z - z_0, x - x_0, \beta - \beta_0) - c_z[\dot{z} - \dot{z}_0] + F_{S_z}, \\ M\ddot{x} &= F_x(z - z_0, x - x_0, \beta - \beta_0) - c_x[\dot{x} - \dot{x}_0] + F_{S_x}, \\ I_{yy}\ddot{\beta} &= T_y(z - z_0, x - x_0, \beta - \beta_0) - c_\beta[\dot{\beta} - \dot{\beta}_0] + F_{S_\beta}, \end{aligned} \tag{2}$$

where z, x, and β are the displacement of the levitating assembly with mass *M* (corresponding to the equilibrium position z_{eq}) and z_0, x_0, and β_0 are the displacement of the base excitation. The nonlinear vertical and horizontal forces F_z and F_x, respectively, as well as the torques T_y are the function of the displacement between the levitating assembly and the base excitation. It is assumed that the viscous damping c_i along the *i*-axis has a 20 percent damping ratio due to eddy current and other energy losses. While the effect of damping is not studied in this paper, it is important to note the substantial influence of damping on the stability of the system as it dominates the amplitude of the resonance (Elbuken, Shameli, and Khamesee, 2007). The mass moment of inertia in the out-of-plane *y* axis about the centre of the levitating assembly is given by

$$I_{yy} = m_m \left[\frac{1}{2}(be)^2 + \frac{1}{4}(cp + c)^2\right], \quad (3)$$

in which m_m = 0.45 kg is the mass of the single top magnet. F_{S_i} refers to the active control force required in the *i*-axis for stable operation.

To eliminate the need of active stability control forces in the vertical *z* and rotational *β* DOFs (i.e., $F_{S_z} = F_{S_\beta} = 0$), the equilibrium position z_{eq} is chosen to be 10 mm below the QZS position (vertically stable) and gap *p* to be greater than or equal to one (rotationally stable). For simplicity, a proportional controller K_p is used to provide additional stiffness to the passively unstable horizontal *x* DOF, and is given by

$$F_{S_x} = -K_p(x - x_0),$$
$$K_p = N \times |k_{xx}|, \quad (4)$$

where *N* is the gain weighting. Theoretically, without any cross-coupling and base excitation, the spring should be levitating stably with *N* > 2 (i.e., for stability, the resulting stiffness must be greater than zero). Subsequent analyses however showed that there exist strong coupling between the horizontal and rotational DOFs; the minimum gain weighting *N* required for stable levitation is inversely proportional to the horizontal gap *p*.

3.2.1 Case 1: Initial perturbation with no base excitation

Before proceeding to more complex dynamic simulations involving base excitation, it is desired to find the combination of horizontal gap *p* and gain weighting *N* that may possibly gives stable levitation at resonance. For this purpose, the system is simulated with the dynamics seen in Eqn. (2) with $z_0 = x_0 = \beta_0 = 0$ and a small perturbation in the vertical *z* DOF using Matlab's ode45 solver.

Figure 3 shows the minimum gain weighting *N* (0.1 precision) required to stabilise the levitating assembly at the chosen equilibrium position z_{eq} after an initial perturbation of $z_{eq}/2$ for a given gap *p*. The design criterion includes a steady-state error of less than 2 percent for a simulation time of 100 s. The simulation time corresponds to a complete sweep of swept sine signals for the next case; it is important to choose an appropriate simulation time as the results would vary accordingly (Kamaruzaman et al., forthcoming). Table 1 shows the combination of gap *p* and gain weighting *N* used for the subsequent cases.

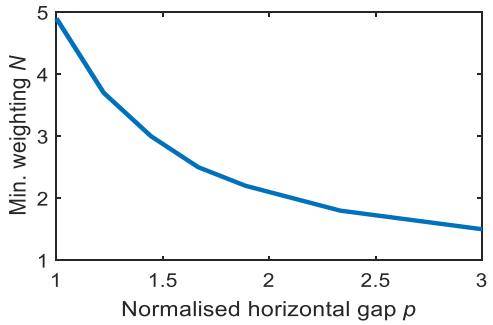

Figure 3: Minimum proportional gain weighting *N* for varying gap *p* from 1 to 3 (10 points linearly spaced).

Table 1: Gap *p* and gain weighting *N* retrieved from Figure 3.

Horizontal gap *p*	Gain weighting *N*
1.00	4.9
1.44	3.0
1.89	2.2
2.33	1.8
2.78	1.6

3.2.2 Case 2: 1-DOF swept sine and tonal base excitation

To identify the natural frequencies and the vibration response of the system due to the identified gap *p* and gain weighting *N*, the system is subjected to a 1-DOF swept sine base excitation of amplitude A_e from 0.1 to 25 Hz with a fixed time step of 4 ms for a sweep time of 100 s – each DOF is excited individually, not simultaneously.

In order to determine suitable excitation amplitude A_e for each DOF, a while loop that increments the amplitude by 0.1 mm (for the translational DOFs) and 0.1° (for the rotational DOF) before instability occurs is used. For a

gap of p = 1 and gain weighting N = 4.9, it is found that the maximum allowable excitation amplitudes for stability are 5.6 mm, 1.1 mm, and 8.8° for the vertical z, horizontal x, and rotational β DOFs respectively.

Using a gap of p = 1 and gain weighting N = 4.9, Figure 4 shows the vibration transmissibility T_{ij} of the system for a range of base excitation amplitudes A_e, where i and j represent the direction (DOF) of the input base excitation and output mass displacement, respectively. For the vertical z DOF base excitation, it is seen that the peak of the resonance of the transmissibilityT_{zz} (Figure 4(a)) shifts to a lower frequency region as the excitation amplitude increases. This indicates that the stiffness characteristic of the system changes as it is displaced further away from the equilibrium position (i.e., increasing nonlinearity). Figure 4(b) shows that the vertical base excitation does not affect the vibration response in the horizontal x DOF, indicating no cross-coupling between the axes. This is expected as the system is vertically symmetric. A similar trend is observed for the transmissibility $T_{z\beta}$.

Interesting vibration response is seen in Figure 4(c) for the horizontal x DOF base excitation, where there exist two resonances of similar magnitude for the transmissibility T_{xx}. The first resonance emerges due to the strong cross-coupling between the horizontal x and rotational β DOFs. It is observed that only the cross-coupling resonance is affected by the change in the excitation amplitude A_e. This may attributed to the fact that the magnets are much bigger compared to the range of horizontal displacement. The vertical z DOF of the levitating assembly is not largely affected by the horizontal base excitation. Similarly, two peaks are seen in Figure 4(e) for the rotational β DOF base excitation; however, the cross-coupling resonance is not as of great concern as the magnitude is much smaller compared to the direct (primary DOF) resonance.

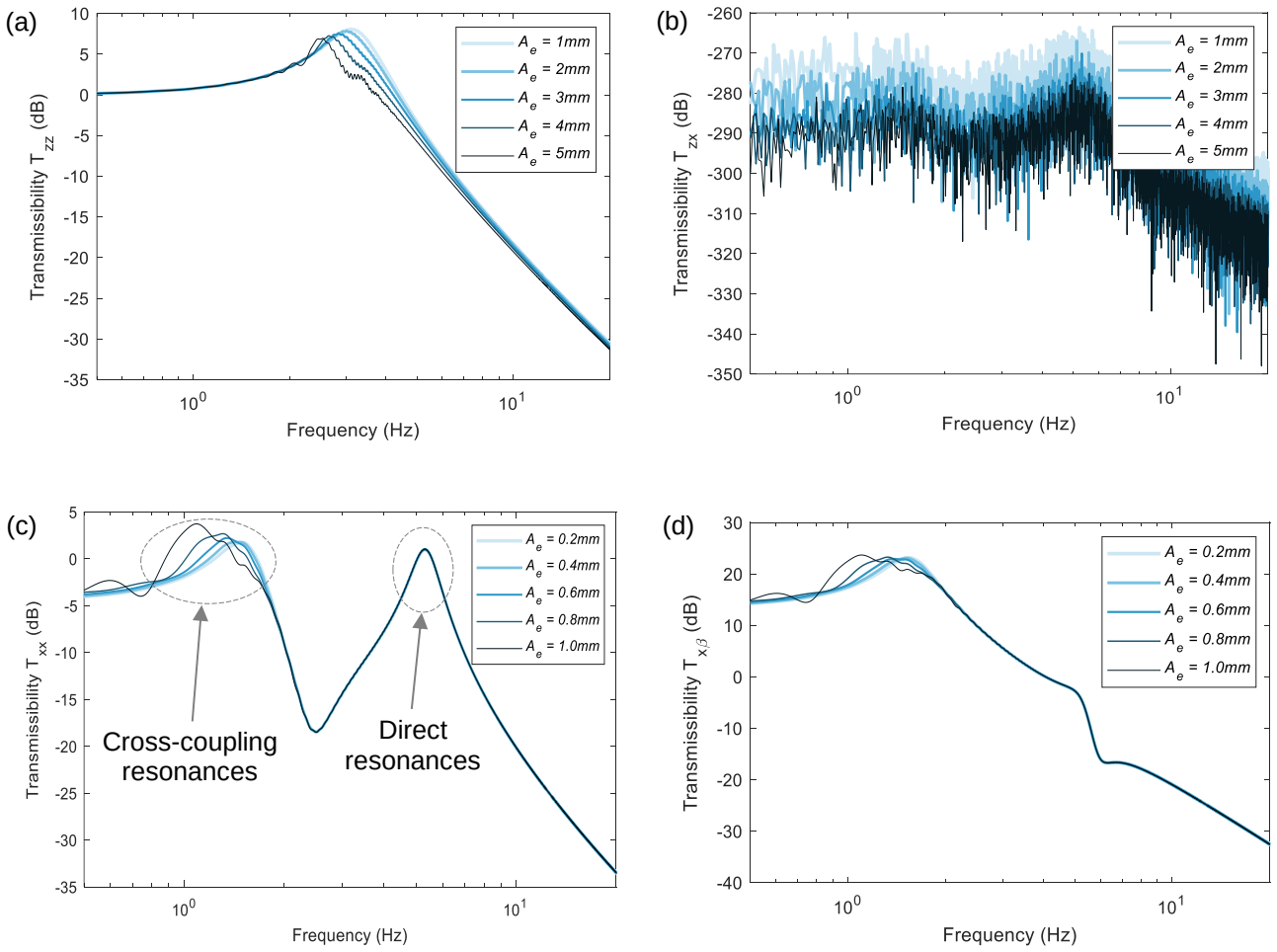

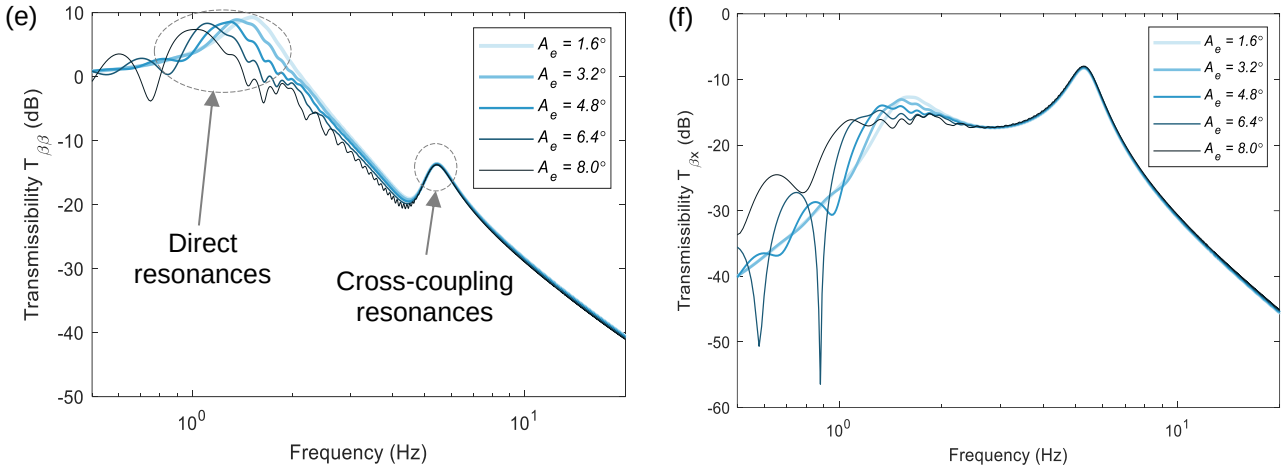

Figure 4: Vibration transmissibilities due to 1-DOF swept sine base excitation. (a) Transmissibility T_{zz}. (b) Transmissibility T_{zx}, which is composed of numerical noise. (c) Transmissibility T_{xx}. (d) Transmissibility $T_{x\beta}$. (e) Transmissibility $T_{\beta\beta}$. (f) Transmissibility $T_{\beta x}$. (FFT properties: 25000 NFFT, 10 averages, no window, 250 Hz sampling frequency).

To further examine the system nonlinearity, the system is subjected to an individual (not simultaneously) tonal sine wave base excitations of amplitude A_e and resonance frequency as seen in Figure 4 correspondingly. The excitation at resonance was chosen so as to attain greatest mass displacement, and thus achieved greatest nonlinearity (Robertson et al., 2009). Figure 5 illustrates the phase plot of the system subjected to such excitation for a range of amplitudes A_e, where the dotted line represents the corresponding linear response. Two phase plots are obtained for both the horizontal x and rotational β DOFs, one for the direct (primary) resonance while the other for the cross-coupling resonance.

For the vertical z DOF, the phase plot of the nonlinear system is very similar to its equivalent linear representation for small amplitude excitations. However, as the amplitude increases, the response of the nonlinear system becomes slower compared to that of the linear system. This shows that the nonlinearity increases with the excitation amplitude, which is anticipated as the displacement of the levitating assembly from the equilibrium position is proportional to the excitation amplitude. The increased nonlinearity is also observed for the horizontal x and rotational β DOFs, but the difference between the phase plots of the nonlinear system and its linear representation is more apparent, indicating that the two DOFs are highly nonlinear. This highlights the need for a full nonlinear simulation instead of a linear one as the latter fails to capture the dynamics of the system accurately.

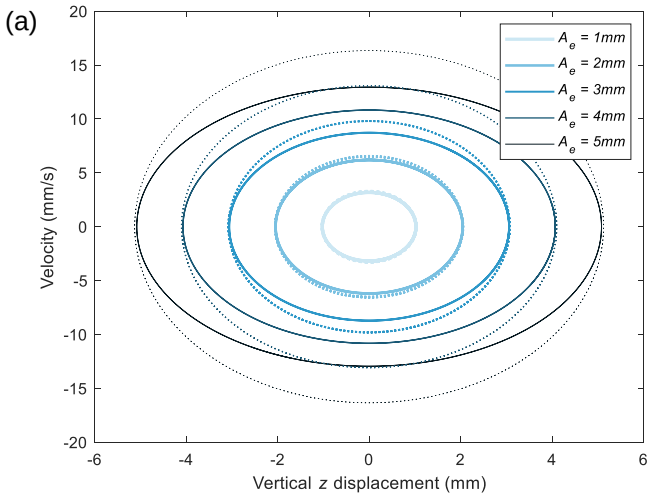

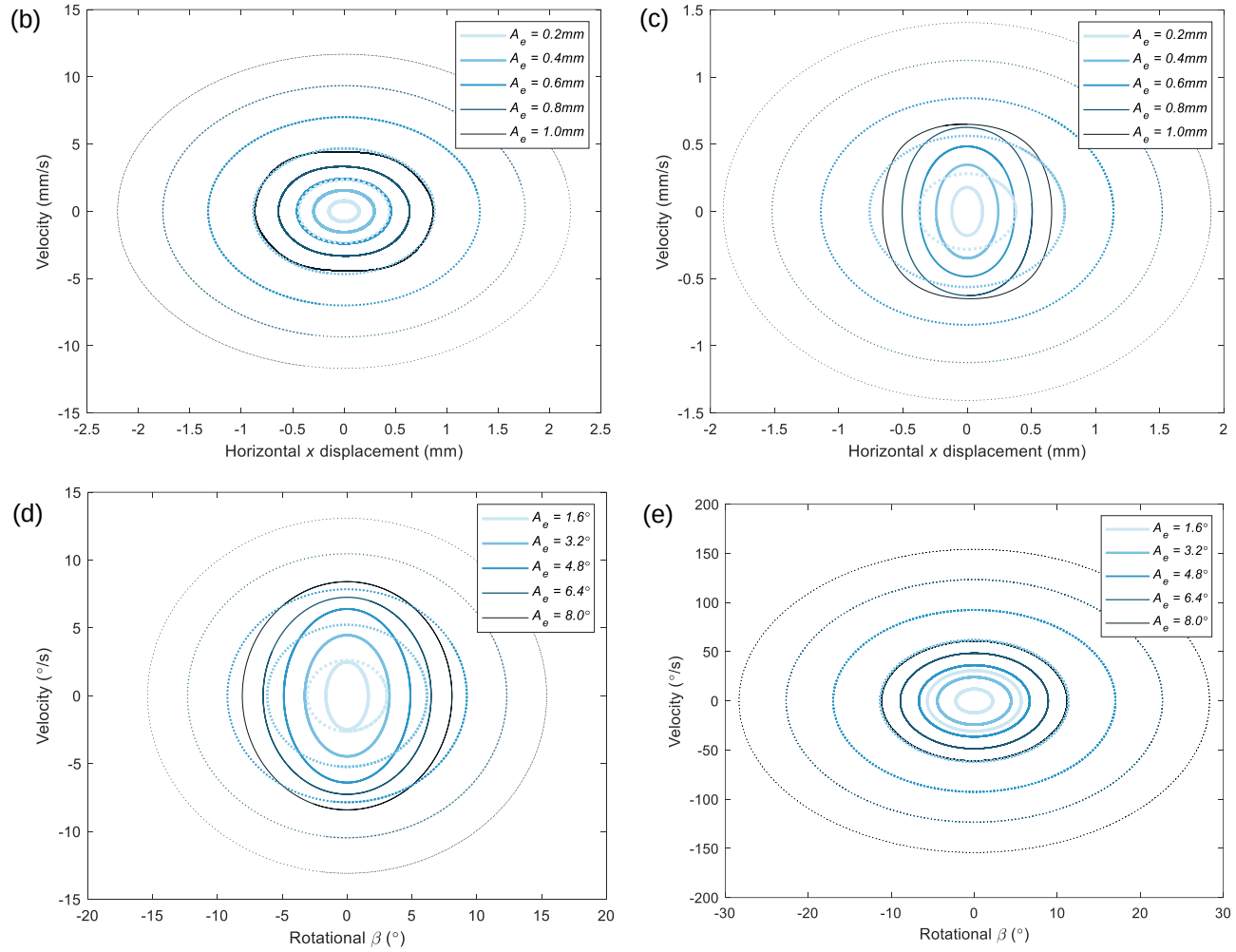

Figure 5: Phase plot of the system with sine base excitation of varying amplitude A_e. Solid and dotted lines represent the system and its equivalent linear system, respectively. (a) Vertical excitation. (b) Horizontal excitation with primary resonances. (c) Horizontal excitation with cross-coupling resonances. (d) Rotational excitation with primary resonances. (e) Rotational excitation with cross-coupling resonances.

3.2.3 Case 3: 3-DOF uniform random base excitation

In order to depict the influence of the horizontal gap p on the vibration isolation performance of the system, it is important to consider a full (3-DOF) base excitation. For this purpose, the system is excited with uniformly distributed random noise, where the bound of the excitation amplitude for each DOF is shown in Table 2. These amplitudes were determined iteratively as the largest in the range tested previously was found to cause instability in the system when excited in all degrees of freedom simultaneously.

Table 2: Amplitude bound for random base excitation.

DOF	Amplitude
z	$\pm$ 3.0 mm
x	$\pm$ 0.6 mm
β	$\pm$ 4.8°

Figure 6 shows the vibration response of the system due to such base excitation for varying sets of horizontal gap p and gain weighting N. The results indicate that the vertical z DOF is not influenced by the change in stiffness characteristics in the other two DOFs, which matches our earlier finding (Figure 2). Therefore, if it is desired to shift the resonance towards the lower frequency region, only the equilibrium position is of our concern. However, changing the equilibrium position closer towards the QZS position would result in generating new combination of gap p and gain weighting N as the stiffness characteristics of both the horizontal x and rotational β DOFs vary. Hypothetically, as the equilibrium position moves closer to the QZS position, the instability in the horizontal x DOF would reduce; thus, less stability control effort would be required. The hypothesis will be examined in future work.

It is seen that for the horizontal x and rotational β DOFs, there exists a trade-off between their isolation performance – for the horizontal x DOF, the vibration isolation response is best with the combination of gap p = 1 and gain weighting N = 4.9. However, the vibration response of the rotational β DOF is worst with such combination. Therefore, appropriate combination of gap p and gain weighting N must be chosen based on one's requirements.

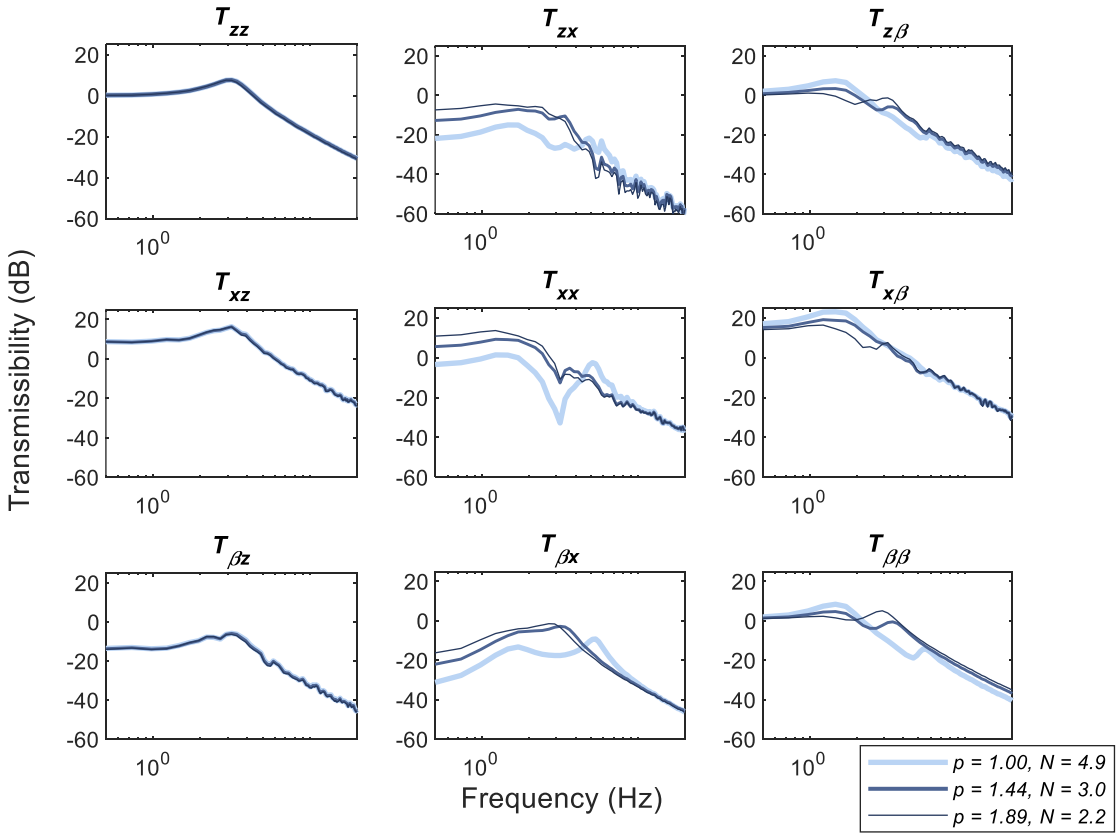

Figure 6: Vibration transmissibilities of the system in all 3 DOFs including cross-coupling response. (FFT properties: 2^{10} NFFT, Hanning window, 50 percent overlap, 250 Hz sampling frequency).

4 CONCLUSIONS

In this paper, the influence of the lever arm (horizontal gap p) on the stability and vibration isolation performance of a planar quasi-zero stiffness magnetic spring subjected to base excitation was investigated. Several combinations of gap p and gain weighting N (active control effort in the horizontal x DOF) that give stable levitation when subjected to a small initial perturbation in the vertical z DOF were identified, which served as a basis for examining the effects of such parameters on the vibration response of the system.

A set of gap p = 1 and gain weighting N = 4.9 was chosen to investigate the system nonlinearity due to varying excitation amplitude, in which it was observed that the system nonlinearity in the vertical z DOF increases with

the excitation amplitude. The horizontal x and rotational β DOFs show similar trend but with higher nonlinearity and cross-coupling. The system therefore must be simulated with full nonlinear simulation as linear simulation would lead to incorrect response.

A full random base excitation of the system with three sets of gap p and gain weighting N revealed that the parameters only affect the horizontal x and rotational β DOFs. A trade-off between the vibration isolation performance for the two DOFs were however seen. Thus, the parameters must be carefully selected based on the system requirements. Future work includes experimental validation, as well as investigation of the influence of the equilibrium position and damping on the stability and vibration response of the system.

REFERENCES

Akoun, G., and J. P. Yonnet. 1984. "3D analytical calculation of the forces exerted between two cuboidal magnets." *IEEE Transactions on Magnetics* 20 (5): 1962-1964. doi: 10.1109/TMAG.1984.1063554.

Bassani, R. 2006a. "Earnshaw (1805-1888) and passive magnetic levitation." *Meccanica* 41 (4): 375-389. doi: 10.1007/s11012-005-4503-x.

Bassani, R. 2006b. "Levitation of passive magnetic bearings and systems." *Tribology International* 39 (9): 963-970. doi: https://doi.org/10.1016/j.triboint.2005.10.003.

Choi, K-B., Y. G. Cho, T. Shinshi, and A. Shimokohbe. 2003. "Stabilization of one degree-of-freedom control type levitation table with permanent magnet repulsive forces." *Mechatronics* 13 (6): 587-603. doi: 10.1016/s0957-4158(02)00032-6.

Earnshaw, S. 1839. "On the nature of the molecular forces which regulate the constituition of luminiferous ether." *Transactions of the Cambridge Philosophical Society*: 97-112.

Elbuken, C., E. Shameli, and M. B. Khamesee. 2007. "Modelling and analysis of eddy-current damping for high-precision magnetic levitation of a small magnet." *IEEE Transactions on Magnetics* 43 (1): 26-32. doi: 10.1109/TMAG.2006.885859.

Kamaruzaman, N. A., W. S. P. Robertson, M. H. Ghayesh, B. S. Cazzolato, and A. C. Zander. Forthcoming. "Improving passive stability of a planar quasi-zero stiffness magnetic levitation system via lever arm." 2018 IEEE International Magnetics Conference (INTERMAG), Singapore, 23-27 April 2018.

Robertson, W. 2013. "Modelling and design of a magnetic levitation systems for vibration isolation." Doctor of Philosophy Thesis, School of Mechanical Engineering, The University of Adelaide.

Robertson, W., B. Cazzolato, and A. Zander. 2012. "Theoretical analysis of a non-contact spring with inclined permanent magnets for load-independent resonance frequency." *Journal of Sound and Vibration* 331 (6): 1331-1341. doi: http://doi.org/10.1016/j.jsv.2011.11.011.

Robertson, W., M. R. F. Kidner, B. Cazzolato, and A. Zander. 2009. "Theoretical design parameters for a quasi-zero stiffness magnetic spring for vibration isolation." *Journal of Sound and Vibration* 326 (1–2):88-103. doi: http://doi.org/10.1016/j.jsv.2009.04.015.